

A New Algorithm for Radiative Feedback and its Application to the Formation of Massive Stars

Richard Edgar^{1*} and Cathie Clarke¹

¹*Institute of Astronomy, Madingley Road, Cambridge CB3 0HA, Great Britain*

29 October 2018

ABSTRACT

We have developed a simplified method of treating the radiative acceleration of dusty flows. This method retains the sharp impulse at the dust destruction radius that is a feature of frequency dependent radiative transfer, whilst placing minimal demands on computing resources. As such, it is suitable for inclusion in hydrodynamic codes. We have applied this method to the formation of massive stars in spherical geometry, and find that the fraction of a cloud which can accrete on to the central star is a strong function of the Jeans' Number and density profile of the cloud. Massive star formation is favoured by cold homogeneous conditions, as might result in regions where gas is swept up by some external triggering agent. We find (in contrast to previous authors) that massive star formation does not require a depleted dust mixture, although the use of dust at typical interstellar abundances does reduce the final stellar mass compared to cores formed from a depleted mixture.

Key words: stars: formation – stars: early-type – hydrodynamics – methods: numerical – radiative transfer

1 INTRODUCTION

The question of massive star formation ($\gtrsim 10 M_{\odot}$) is of great astrophysical interest. Despite their rarity, massive stars dominate the light from young star clusters. As such, they are important tracers of star formation in distant galaxies. Within the Galaxy, massive stars also have profound effects on their local environment. During their brief lives, massive stars produce an intense UV radiation flux, ionising and dispersing nearby gas (see, e.g. Tenorio-Tagle et al. (1986)), while powerful stellar winds are injected into the surroundings. The death of a massive star is also a dramatic event – a supernova which disperses metals into the interstellar medium, while also injecting a large amount of mechanical energy.

Given this wide range of consequences, it is evidently desirable to understand environmental effects that govern the formation of massive stars. Infall models for low mass stars have been studied for a number of years. Some of the earliest work in the area was performed (independently) by Larson (1969) and Penston (1969). The possibility of magnetic fields was considered by many authors, and ambipolar diffusion has been studied as a means of forming the quasi-static systems often assumed by star formation simulations (see, e.g. Nakano (1979) and Safer, McKee & Stahler (1997)). Infrared excesses of slightly older protostars (e.g.

Mendoza (1968)) are generally interpreted as indicating the presence of accretion discs (see Pringle (1981)). These ideas were drawn together by Shu, Adams & Lizano (1987), and the infall model developed in this paper is now generally accepted for low mass stars. However, massive stars require a more sophisticated treatment.

The shorter evolutionary timescales of massive stars mean that they are likely to join the main sequence before the end of their main accretion phase. This complicates simulations of the core itself – see Tout, Livio & Bonnell (1999) for how this can be a problem even for low mass stars. High accretion rates onto massive cores will also lead to large luminosities, which may significantly affect the accretion flow through radiation pressure on dust grains. Moreover, since the main sequence lifetime of a massive star is comparable to the free fall time of the parent core, it is evident that the accretion history and luminosity evolution may be closely linked throughout the star's life. It should be noted that if stellar masses are self-limited by radiation pressure on dust grains, then the high mass end of the IMF is likely to be highly sensitive to the metallicity and dust grain properties of the parent star forming region. For more details, of these and other problems, see Stahler, Palla & Ho (2000).

The possibility of radiation pressure halting accretion was first considered by Larson & Starrfield (1971). Subsequent work by Wolfire & Cassinelli (1986, 1987) concluded that stars with masses $> 100 M_{\odot}$ could form, provided the dust abundance was depleted from normal galactic values.

* Email: rge21@ast.cam.ac.uk

Wolfire & Cassinelli considered spherically symmetric accretion onto a massive star and modeled the interaction between the stellar/accretion luminosity and the infalling dust. Since interstellar dust typically melts when it reaches a temperature in the range 1500 – 2000 K, there is a significant amount of momentum transfer in a region close to the dust destruction radius, r_d , where the radiation from the central core first impinges on the dusty inflow. Wolfire & Cassinelli used these models to propose several criteria necessary for the formation of massive stars, of which the two most important are

- (i) that accretion should proceed at a sufficiently high rate that the ram pressure at r_d exceeds the pressure associated with the radiation impulse at that point
- (ii) that the ratio of gravitational to radiative acceleration at the outer edge should exceed unity, in order that the initially static material will be set in motion in an inward direction

These criteria have long been held to be inimical to the formation of massive stars and have prompted a range of alternative models, discussed below. The first criterion requires that massive stars form in dense cores ($n \sim 10^6 \text{ cm}^{-3}$ for a $100 M_\odot$ core). This was regarded as uncomfortable because if such case was in a state of hydrostatic support prior to collapse (i.e. if the core contained roughly a Jeans' Mass), the required temperature would be high ($\sim 1000 \text{ K}$ for a $100 M_\odot$ core according to Wolfire & Cassinelli, which is much higher than the temperature in such regions - according to section 3.3 of Garay & Lizano (1999), temperatures are typically $\sim 100 \text{ K}$, rising to a maximum of about 250 K). The second criterion, on the other hand, translates (for a given stellar mass and luminosity) into an upper limit on the permitted value of the flux mean opacity at the outer edge of the core. This turns out to be rather restrictive: for any reasonable value of the radiation temperature at the outer edge, inflow is impossible for the standard dust mixture of Mathis, Rumpl & Nordsieck (1977). Accretion is only permitted if the dust mixture is substantially modified (reduction in the total mass of grains by a factor of four from standard Galactic abundances - a factor of eight was used in their simulations - and a smaller maximum size of the graphite grains). Wolfire & Cassinelli thus concluded that '...special grain conditions must exist for massive star formation to occur.'

These constraints have encouraged the discussion of alternative models of massive star formation. A straightforward and realistic modification of the above is to allow for the angular momentum of the initial core and hence for the breaking of spherical symmetry due to the development of a centrifugally supported disc. Yorke and collaborators (Yorke (1979, 1980), Bodenheimer et al. (1990), Yorke, Bodenheimer & Laughlin (1993), Yorke, Bodenheimer & Laughlin (1995) and Yorke & Bodenheimer (1999)) have pioneered the hydrodynamic study of such a situation, including the effects of radiation pressure on dust. They have pointed out that the problem of massive star formation is considerably eased by the 'flashlight' effect, whereby the bulk of the ultraviolet photons escape along the rotation axis of the disc, and thus do not intercept the accretion flow. For reasons of computational economy, however, the majority of such calculations have been performed using grey (frequency averaged) opaci-

ties to compute the radiative acceleration of the flow. Wolfire & Cassinelli have shown that this simplification may cause the efficacy of radiative feedback to be substantially underestimated (see below). Very recently, Yorke & Sonnhalter (2002) have produced the first 2.5D hydrodynamic simulations in which the acceleration due to radiative feedback is computed using frequency dependent opacities. The complexities of such a code, and the large computational overhead it demands, has meant that it has not yet been possible to explore a large area of parameter space. Hence, it has not been possible to understand fully the relationship between initial conditions and final stellar mass. The continued increase in computational capacity should however bring this problem within grasp in the next few years.

Alternatively, Bonnell, Bate & Zinnecker (1998) have suggested that massive stars form through a mixture of accretion and coalescence in the cores of ultra-dense clusters. Coalescence is an attractive mechanism for massive star formation inasmuch as the effect of radiative feedback is negligible. Nevertheless, in such simulations massive stars also acquire mass through Bondi-Hoyle type accretion and it is unclear how radiative feedback operates for this accretion geometry.

In this paper, we revisit the issue of spherical accretion onto massive stars, through the use of hydrodynamical simulations in which the algorithm for radiative feedback is designed to match the outcome of frequency dependent radiative transfer calculations. We compare the results of such simulations with those of Wolfire & Cassinelli (1987), who constructed *steady* flows on to stars of given mass and luminosity. We find significant differences in the results, in the sense that the conditions for massive star formation are apparently much less restrictive than those envisaged by Wolfire & Cassinelli: in particular, we find there is no need to modify the grain mixture, if collapse occurs from a highly Jeans unstable core. Needless to say, spherical accretion is not a realistic model for massive star formation, but it does represent the geometry in which radiative feedback is likely to be most effective (since both accretion and radiative feedback occur over all solid angles). Since we have shown that the formation of massive stars by accretion is rather unproblematical even in spherical geometry, we may conclude from this that the obstacles to massive star formation are still less severe in the case of realistic (disc) geometries.

The structure of this paper is as follows: Section 2 discusses a simplified algorithm for radiative feedback, which preserves the features of a full frequency dependent treatment. In section 3 we describe the hydrocode modified to include the new algorithm. Results are presented in section 4, and a detailed discussion is in section 5. Conclusions and closing remarks are in section 6.

2 A NEW ALGORITHM FOR RADIATIVE FEEDBACK

One of the most important findings of the radiative transfer calculations of Wolfire & Cassinelli (1987) was that the grey approximation is completely inadequate to describe the physics involved in the dusty inflow. The problem may be seen by comparing figures 6 and 7 of Wolfire & Cassinelli (1987) - the calculations which used the Rosseland mean

opacity completely failed to produce the sharp deceleration at the inner edge of the dust shell. This point is also made by Preibisch, Sonnhalter & Yorke (1995).

The problem stems from the extreme manner in which the dust opacity varies with wavelength - typically $\kappa \propto \lambda^{-1.5}$. Use of the Rosseland mean opacity carries an implicit assumption of thermal equilibrium between the radiation and the fluid. At the inner edge of the dust shell, the dust (melting at ~ 2000 K) encounters the radiation field coming from the stellar surface (at a radiation temperature of $\sim 2 \times 10^4$ K). The assumption of thermal equilibrium is evidently extremely poor at this point in the flow, and the steep variation of the dust opacity with wavelength ensures that this mismatch appears in the dynamics. Figure 8 of Wolfire & Cassinelli (1986) implies that the Rosseland optical depth of the envelope is no more than about 2, but it is easy to show that the optical depth at ultraviolet wavelengths is on the order of hundreds. The use of Rosseland opacities therefore artificially softens the impact of the radiation field.

2.1 The Simplified Model

In order to remedy this situation, we here develop a simplified algorithm which retains the sharp impulse at the inner edge of the dust shell (a feature of the full radiative transfer calculations), whilst at the same time effecting considerable computational economies. The prescription obtained is suitable for incorporation into hydrodynamics codes.

2.1.1 Radiative Transfer

The essence of the method is to follow Wolfire & Cassinelli (1986) in splitting the radiation field into two components: the direct stellar radiation field (L_*) and a diffuse, thermalised field (L_{th}). The total luminosity, comprised of the nuclear luminosity of the core and any accretion luminosity (which both change as the protostar evolves), is conserved, so that

$$L_{\text{tot}} = L_* + L_{\text{th}}$$

at all times and at all radii (when integrated over frequency). The thermalised radiation field may be treated using grey opacities, since figures 6 and 7 of Wolfire & Cassinelli (1987) show that deep within the dust shell, this approximation is valid.

The thermalised radiation field was calculated as follows: At every radius, a photospheric temperature could be defined via

$$L_{\text{th}}(r) = 4\pi r^2 \sigma T_{\text{rad}}^4 \quad (1)$$

The radiation temperature thus obtained is that required to transport the radiative flux, *if the radiation became free streaming at that point*. The optical depth to a potential photosphere at radius r may be calculated as

$$\tau(r) = -\kappa_{\text{R}}(T_{\text{rad}}(r)) \int_{\infty}^r \rho(r') dr' \quad (2)$$

where, κ_{R} is the Rosseland opacity, and for simplicity, it is assumed that no significant reprocessing of radiation occurs outside the potential photosphere. The location of the actual photosphere for the dust shell may then be found by

the conventional definition: a photosphere lies at an optical depth of $2/3$ from infinity.

Outside the photosphere, the value of T_{rad} may be set equal to the radiation temperature of the photosphere, as per the assumption made by equation 2. Inward of the photosphere, the diffusion approximation must be solved:

$$\frac{dT_{\text{rad}}}{dr} = -\frac{3\kappa_{\text{R}}\rho}{4\pi\sigma r^2 T_{\text{rad}}^3} L_{\text{th}}(r) \quad (3)$$

Since the grains are flowing inwards, it is reasonable to assume that they will melt once the radiation temperature reaches $T_{\text{sub}} \sim 2000$ K, permitting the inner edge of the dust shell to be located (see below also).

There remains the question of calculating $L_{\text{th}}(r)$. This can be done by attenuating the stellar radiation field as it proceeds outwards from r_d via

$$L_{\lambda}^*(r) = L_{\lambda}^*(r_d) e^{-\tau_{\lambda}} \quad (4)$$

where

$$\tau_{\lambda} = \int_{r_d}^r k_{\lambda}^{\text{PR}} \rho dr \quad (5)$$

is the wavelength-dependent optical depth of the inflow, and k_{λ}^{PR} is the wavelength dependent radiation pressure opacity, as defined by Wolfire & Cassinelli. There is the potential for this to have an unpleasant effect on equation 3, by affecting T_{rad} . In this case, a slow iterative solution would be required. However, as outlined below, this problem was avoided in the simulations presented.

The mechanical effect of the radiation field is provided using

$$a_{\text{rad}}(r) = \frac{\int k_{\lambda}^{\text{PR}} L_{\lambda}(r) d\lambda}{4\pi r^2 c} \quad (6)$$

which may be calculated separately for the direct and thermalised fields. Since the thermalised field is assumed to be a black body, the integral over wavelength may be calculated in a lookup table of Planck mean opacities.

2.1.2 Dust Physics

The dust physics were brutally pruned, compared to the model of Wolfire & Cassinelli (1987). Instead of following the size evolution of the dust as it was destroyed, the dust is taken to be present or absent, based on its equilibrium temperature in the radiation field. This may be calculated using

$$\frac{1}{(4\pi r_d)^2} \int_0^{\infty} Q^{\text{A}}(a, \lambda) L_{\lambda}^* d\lambda = \int_0^{\infty} Q^{\text{A}}(a, \lambda) B_{\lambda}(T_{\text{sub}}) d\lambda \quad (7)$$

where $Q^{\text{A}}(a, \lambda)$ is the absorption efficiency as a function of wavelength for grains of radius a . The desired sublimation temperature, T_{sub} , grain radius, and grain type may be selected appropriately.

Melting the dust at a set temperature (and, implicitly, having it spontaneously reform at that temperature if outflow occurs) is a gross simplification to the true physical conditions. However, this assumption is often used - see, e.g. Bodenheimer et al. (1990); Preibisch et al. (1993); Bell et al. (1997). It has been calculated in studies of low mass stars (e.g. Krueger, Gauger & Sedlmayr (1994)) that, once conditions are favourable for the formation of dust, the grains

grow rapidly. The caveat is the assertion of Gail & Sedlmayr (1999) that nucleation is a rather difficult process. The appropriate destruction temperature is a matter of some debate. The temperature of 2000 K conventionally quoted is based on the sublimation of graphite grains. However, the dust destruction temperatures quoted by Lenzuni, Gail & Henning (1995) are much lower - typically in the region of 1200 K. Lenzuni et al. suggest that the discrepancy is caused by mistaken assumptions about dust destruction processes. However, Lenzuni et al. found that graphite grains tended to be destroyed by chemispluttering (collisions with hydrogen leading to the formation of short hydrocarbon chains). Only silicates were destroyed by sublimation - and at a much lower temperature. Duschl, Gail & Tscharnuter (1996) present similar calculations for a protoplanetary disk. They also found that graphite grains were destroyed at relatively low temperatures by surface reactions, while the silicates sublimated. However, their silicate grains survive to ~ 2100 K. In the dynamical collapses presented, $T_{\text{sub}} = 1700$ K was used.

In the present work, all dust opacities were calculated from the efficiency tables of Draine. These tables are based on the work of Draine & Lee (1984), Draine & Malhotra (1993) and Laor & Draine (1993), and are updated versions of the values used by Wolfire & Cassinelli. The dust size distribution was taken to be the standard power law of Mathis et al. (1977).

2.1.3 Stellar Radiation

In order to perform the radiative transfer calculation, it is necessary to specify the radiation incident on the inner edge of the dust shell. The spectrum of the stellar radiation field was modified in the manner of Wolfire & Cassinelli (1986), with radiation more energetic than the Lyman Limit reprocessed to lie below it. That is, the stellar spectrum, B_λ^* is chosen such that

$$B_\lambda^* = \begin{cases} 0 & \text{for } 0 < \lambda < 912 \text{ \AA} \\ \epsilon B_\lambda & \text{for } \lambda > 912 \text{ \AA} \end{cases} \quad (8)$$

and

$$\int_0^\infty B_\lambda d\lambda = \int_0^\infty B_\lambda^* d\lambda \quad (9)$$

where B_λ is a true black body spectrum, and ϵ is chosen to ensure equation 9 remains true. Then,

$$L_\lambda^* = 4\pi^2 B_\lambda^* R_*^2$$

2.2 Testing the Simplifications

The approximations described above were tested against the full radiative transfer calculations of Wolfire & Cassinelli (1987). The reference model was the 100 M_\odot calculation of Wolfire & Cassinelli (1987). This model had a steady accretion rate of $5 \times 10^{-3} M_\odot \text{ yr}^{-1}$ and a total core luminosity of $2.43 \times 10^6 L_\odot$. Where possible, boundary conditions were taken to be those specified by Wolfire & Cassinelli, so equation 7 was not used. Use of these boundary conditions also eliminated the troublesome relation between equations 3 and 4, since the dust would always be destroyed in the innermost grid cell.

The gas equation of motion was modified to be

$$\frac{1}{2} \frac{du^2}{dr} = -\frac{GM(r)}{r^2} - \frac{1}{\rho} \frac{dP}{dr} + \frac{\int k_\lambda^{\text{pt}} L_\lambda(r) d\lambda}{4\pi r^2 c} \quad (10)$$

where $M(r)$ is the mass enclosed at radius r , and P is the gas pressure. The λ subscripts indicate quantities that are wavelength dependent. This is based on equation 31 of Wolfire & Cassinelli (1987). However, the left hand side has been changed into a ram pressure gradient, while the dust to gas mass ratio (which is $\sim 10^{-5}$) has been dropped from the right hand side.

The steady state velocity field obtained is plotted in Figure 1. It may be seen that, although the general behaviour has been duplicated, there is a discrepancy of a few kilometres per second in the inner portions of the flow. This difference can probably be ascribed to the extremely approximate nature of the radiative transfer method used. Since the dust shell has an optical depth of the order unity at temperatures appropriate to the diffuse field, it is inevitable that errors will creep in - this regime is notoriously tricky to approximate. While it is certain that some method could be concocted to improve this specific case, its generality would be suspect. It should be noted that the magnitude of the jump in the inflow velocity at the inner edge of the dust shell is identical to that of Wolfire & Cassinelli (1987). Comparing the momentum fluxes of the curves, the initial encounter with the stellar radiation gives a change equivalent to $0.96L/c$, while the thermalised field adds another $0.71L/c$. These numbers are as one might expect - all the luminosity¹ is absorbed and re-emitted at the inner edge of the dust shell. However, the thermal processing is significant, contributing almost as much momentum flux as the initial strike. Again, this is as one would expect, given that the entire shell has $\tau_R \sim 1$.

The algorithm presented is a substantial improvement over calculations using only the Rosseland mean (which cannot even reproduce the *qualitative* behaviour of the inflow). Although there is a discrepancy of a few km s^{-1} at the inner edge of the dust shell, we note that the regime under consideration was the most problematic to approximate, with Rosseland optical depths only slightly larger than unity. We would expect the approximations we have made to become better as the dust shell becomes optically thicker.

3 THE DYNAMICS CODE

The ZEUS-2D code of Stone & Norman (1992) was chosen to simulate the collapses. Since the flows were generally found to be highly supersonic, and fairly optically thin in the Rosseland mean, the gas equation of state was taken to be isothermal, with the temperature set at the start of the simulation.

Resolution considerations lead to a slight modification of the algorithm detailed in section 2. The loop between equations 3 and 4 was broken by noting that the flow is likely to be so optically thick that the direct stellar field will be attenuated in a single grid cell. In this case, $L_{\text{th}}(r) = L_{\text{tot}}$

¹ The missing four percent is probably due to the changing velocity affecting the density structure (since the accretion rate is constant), which will then change the gravitational forces slightly

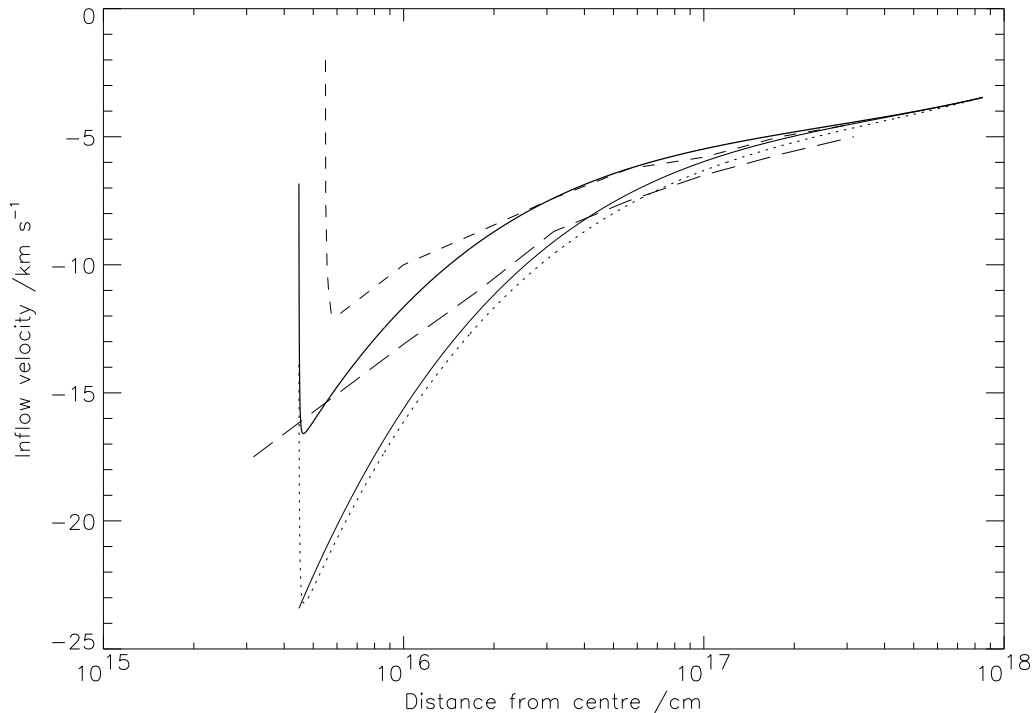


Figure 1. Inflow velocities onto $100 M_{\odot}$ core. The thick solid curve is that obtained from the new algorithm, while the thin solid curve is the freefall solution. The dashed curves are points read from Wolfire & Cassinelli (1987), with the short dashes following the full solution of their figure 6, while the long dashes follow the Rosseland mean calculation of their figure 7. The dotted line is the curve one obtains if the effects of L_{th} are omitted in the new algorithm

outside this grid cell. The mechanical impulse exerted on the inflow at the dust destruction radius may be represented by the injection of L_{tot}/c of momentum into the dust destruction grid cell. If a photosphere is not found according to equation 2, then the value of r_d may be calculated using equation 7 and the stellar field swept outwards from this point using equation 4. No thermalised field need be calculated in this case, since its effect will be minimal.

To avoid the central grid cell reaching unreasonable densities (and thereby consuming impractical amounts of computer time), ZEUS was modified so that a linearly decreasing amount of mass was accreted from the innermost grid cells, and placed into a point mass at the centre of the grid. This simulated the formation of the protostar - which is not resolved in our work. The number of cells which were permitted to accrete, and the maximum fraction accreted were found to have little effect on the results. The point mass was used to determine the intrinsic luminosity and the radius (for the accretion luminosity) of the forming protostar. These quantities were determined using the Zero Age Main Sequence (ZAMS) formulae of Tout et al. (1996).² To allow for the fact that the core would not immediately settle to its main sequence radius, the method of Yorke (1979) was adopted: once the core reached $0.1 M_{\odot}$, its radius was set equal to that of the first grid cell. It was then allowed to contract on its instantaneous Kelvin-Helmholtz timescale,

until it shrank to its main sequence radius. It is of course undesirable for the physical behaviour to be determined by computational considerations (the positioning of the grid cell). However, tests at different resolutions found no significant variation in behaviour due to this.

Most runs were performed with a grid of 600 cells, fifty of which were concentrated in the inner 100 au with linear spacing. The remainder were logarithmically spaced. Higher resolution runs were also performed, typically with 800 grid cells following the same general distribution pattern.

4 RESULTS

Two sets of simulations were performed. The first started from uniform initial conditions, the second started from a power law density profile.

4.1 Collapse from Uniform Initial Conditions

In Tables 1, 2 and 3 we detail a number of simulations which start from uniform initial density. The initial density was $10^{-19} \text{ g cm}^{-3}$, with the different masses obtained by varying the simulation volume. The temperature of the gas, T_{gas} of each run was fixed at the indicated temperature; the corresponding value of α is also listed, where α was defined as

$$\alpha = \frac{E_{\text{th}}}{|E_{\text{grav}}|} \quad (11)$$

² Note that this assumption will overestimate the luminosity of the core, and increase the effects of radiative feedback

T_{gas}/K	α	M_*/M_{\odot}	Comments
10	0.03	196	No thermalised field
200	0.54	88	No thermalised field
10	0.03	185.7	
10	0.03	188.3	High resolution
10	0.03	183.8	High resolution
20	0.06	172.6	
50	0.14	126.5	
100	0.27	84.4	
150	0.41	67.1	
200	0.54	48.7	
200	0.54	47.7	High resolution
300	0.81	39.9	
400	1.08	45.1	
10	0.03	137.1	Normal dust levels
10	0.03	138.4	Normal dust levels, high resolution
20	0.06	106.4	Normal dust levels
50	0.14	54.5	Normal dust levels
100	0.27	15.8	Normal dust levels
150	0.41	13.6	Normal dust levels
200	0.54	12.7	Normal dust levels
300	0.81	12.3	Normal dust levels
400	1.08	12.4	Normal dust levels
400	1.08	11.7	Normal dust levels, high resolution

Table 1. Results from 241 M_{\odot} collapses of uniform gas

where E_{grav} is the system gravitational energy and

$$E_{\text{th}} = \frac{3\mathcal{R}MT_{\text{gas}}}{2\mu}$$

where \mathcal{R} is the molar gas constant.³ Note that by setting $c_v = \frac{3}{2}\mathcal{R}$ the freeze-out of the rotational modes of molecular hydrogen is ignored. However, this is appropriate to the isothermal nature of the simulations. Unless stated otherwise, the dust mixture is the depleted one employed by Wolfire & Cassinelli (1987). The ‘normal’ dust mixture is that of Draine & Lee (1984), which is used by Wolfire & Cassinelli (1986). Some of the simulations had no thermalised radiation field present (that is, $L_{\text{th}} = 0$ everywhere), as indicated. It should be noted that these runs lead to higher final stellar masses than their counterparts with the full feedback mechanism, pointing to the importance of the reprocessed radiation. Variation of the grid resolution was not found to have a significant impact on the final stellar masses.

Figures 2, 3, 4 and 7 depict snapshots of the flow profile and illustrate the chief phases of the collapse of homogeneous clouds subject to radiative feedback. In all cases, a core forms after a free-fall time, where

$$t_{\text{ff}} = \sqrt{\frac{3\pi}{32G\rho_0}} = 2.1 \times 10^5 \left(\frac{\rho_0}{10^{-19} \text{ g cm}^{-3}} \right)^{-\frac{1}{2}} \text{ yr}$$

which is the standard result for the pressure free collapse of a homogeneous cloud. There is obviously no core luminosity (or feedback applied) up to the point of core formation. The density profile during the initial collapse depends on the temperature of the flow: warmer flows exhibit the

T_{gas}/K	α	M_*/M_{\odot}	Comments
10	0.05	64.0	
20	0.11	56.0	
50	0.27	40.5	
100	0.54	30.2	
150	0.81	26.5	
200	1.08	26.8	
300	1.62	-	Did not collapse
10	0.05	37.6	Normal dust levels
20	0.11	23.7	Normal dust levels
50	0.27	12.2	Normal dust levels
100	0.54	11.5	Normal dust levels
150	0.81	14.2	Normal dust levels
200	1.08	11.8	Normal dust levels
300	1.62	-	Normal dust levels, did not collapse

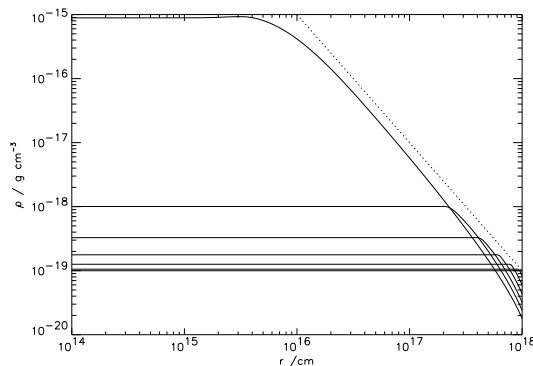
Table 2. Results from 88 M_{\odot} collapses of uniform gas

T_{gas}/K	α	M_*/M_{\odot}	Comments
10	0.003	4809	No thermalised field
200	0.067	3976	No thermalised field
10	0.003	4368	
200	0.067	2373	

Table 3. Results from 5630 M_{\odot} collapses of uniform gas

behaviour discussed by Larson (1969) and Penston (1969) - a flat central density profile with r^{-2} wings (Figure 2). The colder collapses produce larger constant density regions as they approach homologous collapse, with steeper wings (typically closer to r^{-3} , see Figure 3).

Once the core has formed, the inner region of the flow, which is dominated by the core’s gravity, approaches the $r^{-1.5}$ profile expected for steady flow onto a point mass (Figure 4). At this stage, the dominant contribution to the core luminosity is initially from accretion, but the relative importance of the intrinsic core luminosity increases as the core mass grows (Figure 5). In the final phase of the evolution, the accretion flow starts to be modulated by the effect of radiative feedback on the dust - oscillations in the accretion rate may be seen in Figure 6. Radiation pressure temporarily reduces the flow rate from the dust destruction radius, which produces a drop in the accretion rate onto the core after one freefall time from r_d . The corresponding drop in luminosity

**Figure 2.** Initial collapse of 200 K 241 M_{\odot} cloud. The curves are plotted for $t = 0$ and after 0.17, 0.34, 0.51, 0.69, 0.84, and 1.0 freefall times. Dotted line is r^{-2} curve

³ Note that with this definition, α is related to the Jeans’ Number, N_J by $N_J = \alpha^{-\frac{3}{2}}$

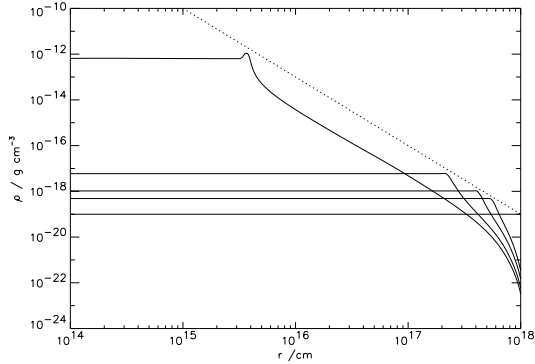


Figure 3. Initial collapse of 10 K $241 M_{\odot}$ cloud. The curves are plotted for $t = 0$ and after 0.76, 0.84, 0.94 and 1.0 freefall times. Dotted line is r^{-3} curve

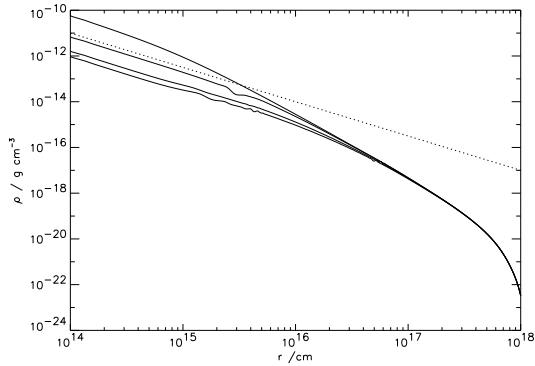


Figure 4. Middle phase of collapse of 10 K $241 M_{\odot}$ cloud. The core grew from $101 M_{\odot}$ to $156 M_{\odot}$ during the period of 381 yr plotted. Dotted line is $r^{-1.5}$ curve

causes a reduction in feedback at r_d , and the accretion rate climbs again. The effect of this time delayed feedback is imprinted as oscillations in the density profile (Figure 7). In the last profile, the large drop in density at the inner edge of the dust shell is plainly visible, as the flow is effectively stalled by the momentum imparted by the photon field.

At a quantitative level, the behaviour of the flow can

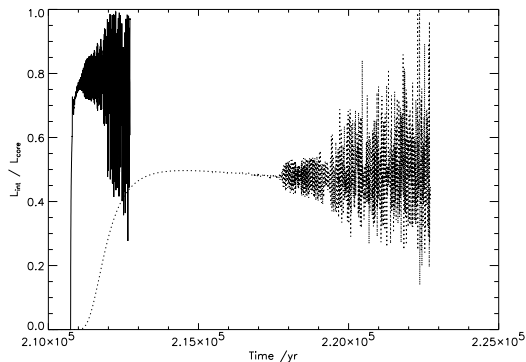


Figure 5. Comparison of intrinsic (nuclear) luminosity to total core luminosity for 10 K (solid line) and 200 K (dotted line) $241 M_{\odot}$ clouds

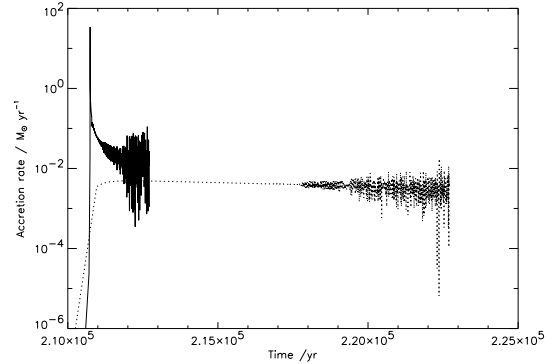


Figure 6. Accretion rates for 10 K and 200 K $241 M_{\odot}$ clouds. Solid line is for 10 K gas, dotted line follows 200 K cloud

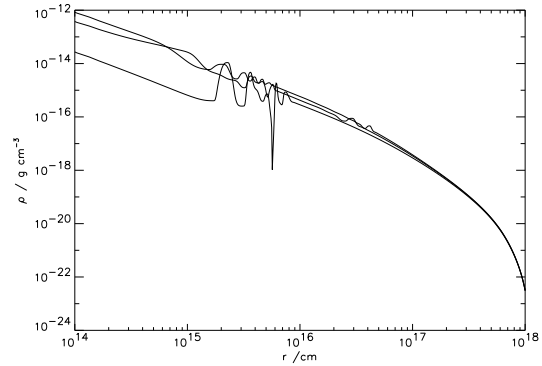


Figure 7. Terminal phase of collapse of 10 K $241 M_{\odot}$ cloud. This plot covers a period of 1200 yr at the end of the simulation

be understood in terms of the analytic expressions presented in Appendix A. In particular, accretion is found to stall at the point where the momentum flux in the accretion flow at r_d matches L/c from the core. The evolution of the dust destruction radius (computed in the code according to the algorithm of section 2) may be compared with the approximation $L = Ar_d^2$ made in the Appendix, and was found to be in satisfactory agreement over most of the evolution. Values of A were found to be similar to those of Wolfire & Cassinelli (1987).

As Figure 6 demonstrates, the colder gas clouds underwent a spike of accretion as shells from a range of radii arrive almost simultaneously at the centre (as expected for a homogeneous collapse). Roughly half the mass of the cloud goes into the core during this first spike. The associated accretion rate is high, and briefly super-Eddington - see Figure 8.⁴ For a star of mass $M M_{\odot}$, the Eddington Luminosity is $3 \times 10^4 M L_{\odot}$. After the initial accretion spike, accretion continued but soon large oscillations develop in the accretion rate, and accretion subsequently stalls.

The ‘warm’ run behaves somewhat differently. The ac-

⁴ Note that our simulation takes no account of electron scattering opacity, since the ionised regions of the flow are not resolved. However, since the integrated energy input during the super-Eddington phase is rather less than the binding energy of the core, the core would not be liable to disruption

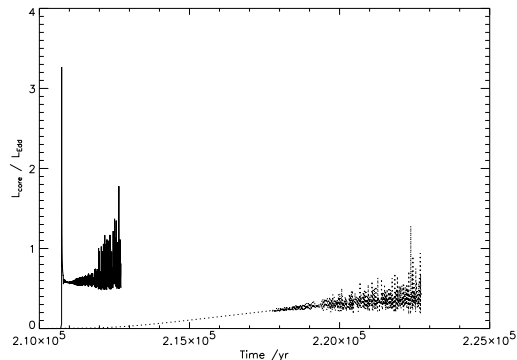


Figure 8. Comparison of total luminosity to Eddington luminosity for 10 K (solid line) and 200 K (dotted line) $241 M_{\odot}$ clouds

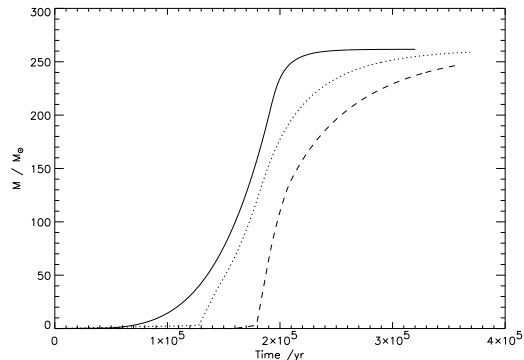


Figure 9. Accretion histories for cloud started from r^{-1} initial density profile and no feedback. Solid curve is for 10 K gas, the dotted line 100 K, and the dashed line 200 K gas

T_{gas}/K	α	M_*/M_{\odot}	Comments
10	0.02	25.3	
20	0.05	28.0	
50	0.11	28.2	
100	0.23	36.3	
150	0.35	51.4	
200	0.46	64.8	
300	0.68	53.2	
400	0.92	45.7	
10	0.02	14.3	Normal dust levels
20	0.05	15.8	Normal dust levels
50	0.11	15.4	Normal dust levels
100	0.23	11.5	Normal dust levels
150	0.35	12.0	Normal dust levels
200	0.46	11.3	Normal dust levels
300	0.68	11.5	Normal dust levels
400	0.92	11.7	Normal dust levels

Table 4. Results from 262 M_{\odot} collapses of $\rho \propto r^{-1}$ gas

cretion rate rises more slowly, and remains steady for about 10% of the freefall time of the original cloud. The rising intrinsic luminosity of the core causes feedback to play an increasing role. Oscillations develop in the accretion rate, leading to the eventual stalling of the accretion flow.

4.2 Collapse from Power Law Initial Conditions

We now consider collapses in which the initial density profile scales as r^{-1} . Final stellar masses as a function of α (still relevant for this density distribution) are given in Table 4. The densities were normalised so that models of given mass and temperature had α values similar to those starting from uniform conditions.

The effect of feedback may be most readily understood by first considering the growth of the central core in such models when feedback is *not* included. A set of sample curves is presented in Figure 9. The core growth of the coldest run roughly follows the $M \propto t^4$ law derived by considering the freefall collapse of thin shells. The core is therefore built over a much longer interval than the homogeneous case. The warmer runs behave in a manner similar to their homogeneous counterparts, since early core formation is suppressed by the action of pressure gradients. Since $M(r) \propto r^2$, the gravitational acceleration, g , is constant throughout the initial cloud. However, the acceleration due to the pressure

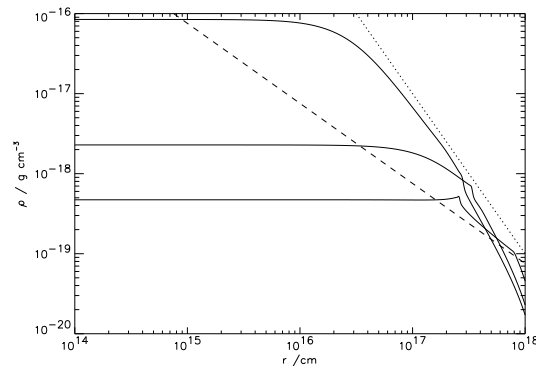


Figure 10. Collapse of 200 K cloud started from r^{-1} initial density profile. The solid curves are plotted for 0.36, 0.72, and 0.86 freefall times from the edge of the simulation. The dashed line is the initial density profile. Dotted line is r^{-2} curve

gradient varies according to

$$\frac{1}{\rho} \cdot \frac{dP}{dr} \sim \frac{1}{\rho} \cdot \frac{P}{r} \sim \frac{c_{\text{iso}}^2}{r} \sim r^{-1}$$

so pressure support improves towards the centre of the cloud. Consequently, the gas evolved towards the Larson–Penston solution initially, as maybe seen from Figure 10. The subsequent behaviour of the warmer clouds closely mirrored those collapsing from uniform initial conditions.

When feedback was included, it was found that the warmest runs led to final stellar masses almost indistinguishable from the corresponding homogeneous simulations (c.f. Tables 1 and 4). This is as one would expect, given the appearance of the Larson–Penston solution prior to core formation. However, for still lower temperatures ($T_{\text{gas}} < 200$ K, or $\alpha < 0.5$ for the conditions considered here), the trend is reversed, and final stellar mass *decreases* with lower temperatures. This behaviour is explained by Figure 9. The lack of pressure support caused the cores to form over a *longer* period of time, since the formation of the core is not delayed by pressure gradients. This permits feedback to operate when a substantial fraction of the initial cloud mass still lies beyond r_{d} .

The interaction of the collapse with the radiative feedback followed a similar pattern to that observed in the col-

lapses from uniform clouds. The collapses with feedback closely followed the behaviour of those without, until the central luminosity became significant. Then, the flow began to oscillate on a short timescale, and accretion halted rapidly.

5 DISCUSSION

Three phases of collapse were observed, where a different physical effect was dominant:

- (i) Self-gravity of the cloud
- (ii) Gravity of the core
- (iii) Luminosity of the core

Stages (i) and (ii) have been studied for a number of years. Radiative feedback is important in the final phase.

A cursory glance at Tables 1, 2 and 3 suggests that, given the right initial conditions, massive stars may form despite the effects of radiative feedback. For example, Table 3 documents the formation of stars containing thousands of solar masses of material; we cannot of course rule out the possibility that such objects would fragment into a cluster of lower mass stars, but this is not a radiative effect. Such stars are not observed, but we find no reason why radiative feedback should prevent their formation. Higher initial cloud masses lead to higher final stellar masses. However, we do find that values of α (defined in equation 11) close to unity cause the fraction of the cloud mass accreted to be very low, whereas small α values gave rise to a high accretion fraction. This variation with α arises because feedback can only become effective in stage (iii) of the collapse. For the colder homogeneous clouds, most of the mass had already arrived within r_d by the time this stage was reached. By contrast, warmer collapses possessed pressure gradients which modified the density profile, and caused the core to form over a more extended period. Indeed, the steady accretion rate of the warm cloud depicted in Figure 6 is rather similar to the conditions considered by Wolfire & Cassinelli (1987), although our differing parameterisations of the protostellar core prevent quantitative comparison. By contrast, the cold collapse is *qualitatively* different and points to the possibility that massive star formation may not be as difficult as previously envisaged.

Wolfire & Cassinelli (1987) concluded that depleted dust abundances were necessary to form massive stars, yet the current work has demonstrated the formation of stars $> 100 M_\odot$ for the Draine & Lee (1984) dust abundances. However, the condition derived by Wolfire & Cassinelli to support this requirement was analogous to the Eddington Limit, and hence was based on accelerations. Balancing accelerations is only useful when the processes involved are close to equilibrium (e.g. radial motion through an accretion disc). The present work studied highly dynamical collapses, and the velocities obtained in the early stages of the collapse were easily sufficient to overcome the net outward acceleration as the luminosity rose.

A plot of initial α against the fraction of mass accreted onto the star (a measure of the efficiency) for an initially uniform cloud is presented in Figure 11. In general, lower α values lead to more massive stars. For $\alpha \sim 1$ and higher dust opacities, the final stellar mass obtained seems to tend

to a constant value (c.f. Tables 1 and 2), possibly indicating that a true radiation pressure limit is being found. For the depleted dust mixture, the stars obtained can still be quite massive – $> 40 M_\odot$.

The results from collapses of $\rho \propto r^{-1}$ gas, as presented in Table 4 show that radiative feedback can be very important under more condensed initial conditions. A plot of α against the star formation efficiency is presented in Figure 12. The rise in efficiency with increasing temperature is plain for the depleted dust, as is the steady value obtained for normal dust abundances. In the case of normal dust abundances, a limit of $\sim 12 M_\odot$ is implied, with the variations around this value not being very significant. For the depleted dust mixture, the rather surprising result that colder gas does not lead to more massive stars is related to the behaviour of the collapse before radiative feedback becomes significant. If thermal effects are significant, they can delay core formation, and hence the onset of radiative feedback. During this delay, gas settled inside the dust destruction radius (see Figure 9 and associated discussion).

6 CONCLUSION

We have developed a new simplified algorithm for calculating radiative feedback in hydrodynamic simulations. This method combines the computational economy of a frequency averaged treatment of the thermalised field (via a modified diffusion approximation) with the benefits of a frequency dependent treatment of the attenuated stellar field. This latter feature ensures that the flow receives the sharp impulse at the dust destruction radius that is found in full radiative transfer calculations; we have demonstrated (Section 2) that this algorithm is significantly superior to methods using grey opacities, which have become the standard method in hydrodynamical simulations to date.

We have applied this algorithm to the formation of massive stars by spherically symmetric accretion. Although this obviously does not represent a realistic geometry for OB star formation, our motivation has been to compare the hydrodynamical treatment of this process with the steady state models of Wolfire & Cassinelli (1987), in order to evaluate how the time-dependence of the hydrodynamic calculation affects the results. Since we find (see below) that massive star formation is rather unproblematical (given appropriate initial conditions), we would expect it to be yet easier with a realistic (disc) accretion geometry. Our chief conclusions are as follows:

- (i) Massive star formation is favoured by models in which the luminous core forms *quickly*. In this case, much of the cloud is already within the dust destruction radius (and hence immune from feedback) when the core luminosity becomes significant. The most favourable conditions involve cold homogeneous collapse, since in this case the core assembly time is shortest. Warmer collapses (with thermal to gravitational energy ratios near unity) produce lower final stellar masses, but can still readily produce OB stars given sufficiently massive progenitor clouds. For these warm collapses, the final stellar masses are rather insensitive to the initial cloud density profile
- (ii) We find that, in contrast to Wolfire & Cassinelli

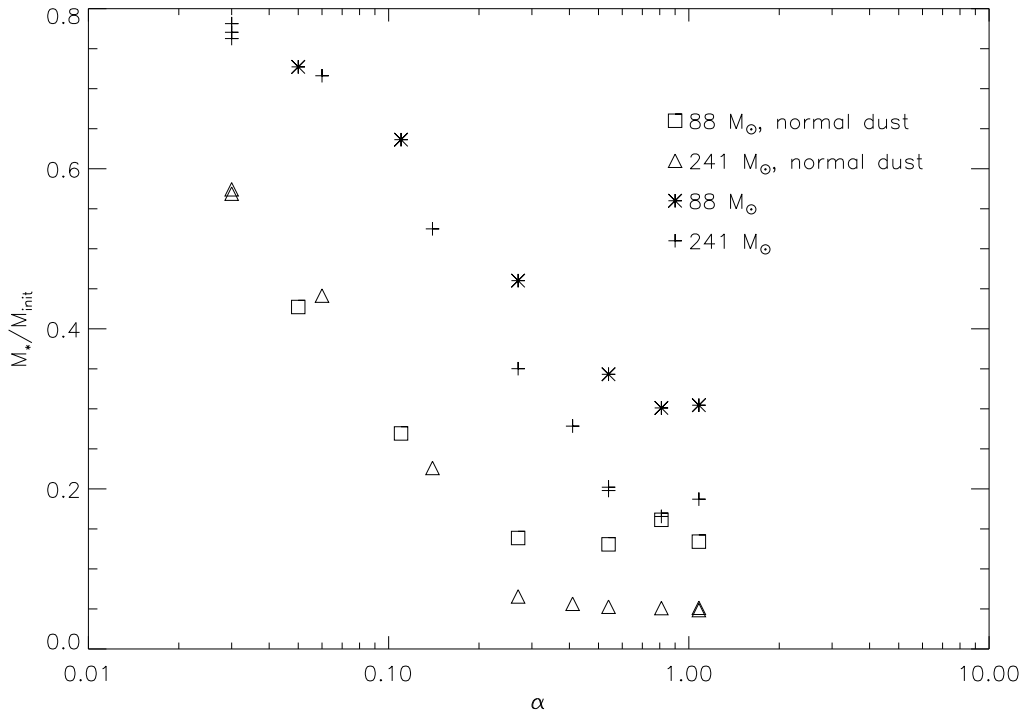


Figure 11. Initial α against final fraction of mass accreted for collapses from a uniform cloud. Note that $N_J \approx \alpha^{-\frac{3}{2}}$ for the uniform collapses

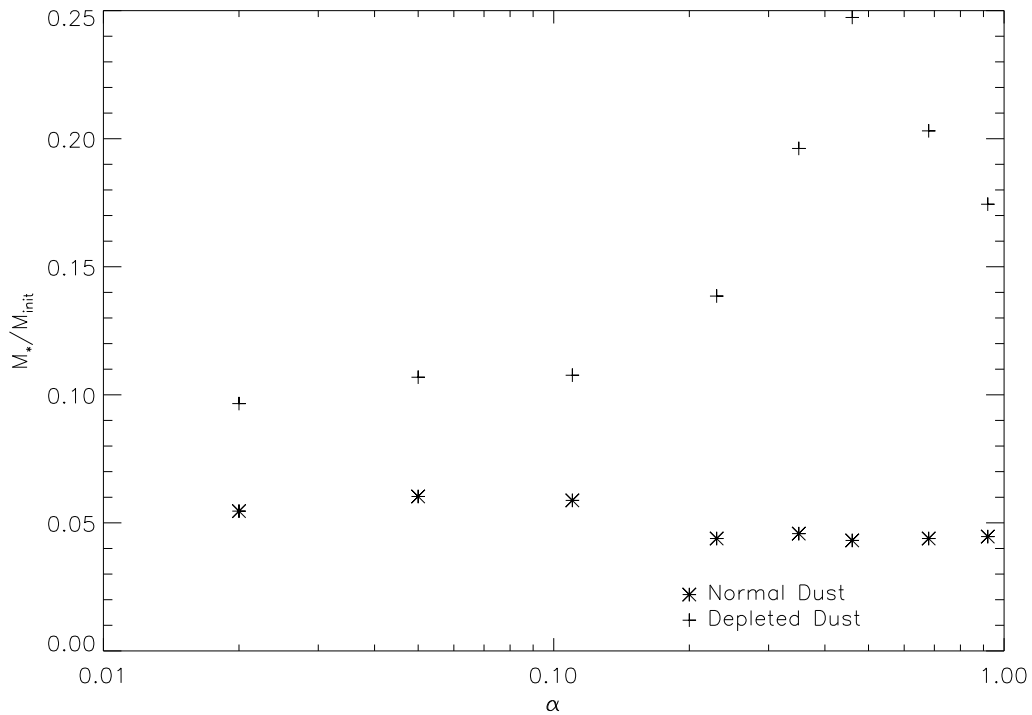


Figure 12. Initial α against final fraction of mass accreted for collapses from an initial density profile of $\rho \propto r^{-1}$. In all cases, the total cloud mass was $262 M_\odot$

(1987), a depleted dust mixture is *not* necessary for the formation of OB stars. The reason for this difference is that Wolfire & Cassinelli required that the net acceleration at the cloud's outward edge was inward, in order to attract the initially stationary material. In the hydrodynamic collapses, the fluid is already inflowing at close to its freefall velocity by the time the core luminosity becomes significant. However, increasing the optical depth implies a stronger deceleration of the flow from the diffuse field, which does reduce the final stellar masses.

Although, as stated above, we do not consider our simulations to be a realistic portrait of massive star formation, we end with a few remarks about the possible relevance of these findings to OB star formation. Firstly, we might expect that the qualitative conclusion that massive star formation is favoured by rapid core formation to hold in other geometries. Such rapid formation is promoted by rather homogeneous, highly Jeans unstable conditions – as might be expected to arise in regions of triggered star formation (see, e.g. Braun et al. (1997) or Olsen, Kim & Buss (2001)). Secondly, we note that in our models in which feedback effects were particularly severe (either due to warm initial conditions or the use of a standard grain opacity), the resulting stellar mass often ended up near to $\sim 12 M_\odot$. The lack of any obvious signature in the IMF around this value therefore argues that the dominant population of progenitor clouds does not fall into this category.

APPENDIX A: SCALING RELATIONS

For accretion to occur, despite radiation pressure on the embedded dust grains, the ram pressure at the dust destruction radius, r_d must exceed the momentum of the radiation field. That is

$$\dot{M}u_d > \frac{L}{c} \quad (\text{A1})$$

where u_d is the inflow velocity at r_d . This is the condition used by Wolfire & Cassinelli (1987) at the inner edge of their dust shell.

The value of u_d may be calculated on the assumption that the stellar mass dominates, and that the material is in free fall at the destruction radius. To make further progress, assumptions must be made about the source of the luminosity.

A1 Luminosity Dominated by Accretion

If the core's luminosity is dominated by accretion, one obtains

$$\dot{M}\sqrt{2GM_*} > \frac{GM_*\dot{M}}{cR_*}r_d^{\frac{1}{2}}$$

To compute the accretion luminosity, a mass-radius relation is required. A simple mass radius relation for massive stars is

$$R_* = \left(\frac{M_*}{M_\odot}\right)^{\frac{3}{5}} R_\odot$$

which leads to

$$r_d < \frac{2c^2R_\odot^2}{GM_\odot^{\frac{6}{5}}}M_*^{\frac{1}{5}}$$

as the condition for accretion. That is, the dust destruction radius must be *less* than some *increasing* function of the stellar mass. This would mean that accretion becomes *easier* over time, and that radiative feedback would place no limit on stellar masses. Evaluating the constants gives the following prediction for steady state accretion to occur:

$$r_d < 4400 \left(\frac{M_*}{M_\odot}\right)^{\frac{1}{5}} \text{ au} \quad (\text{A2})$$

Of course, the dust destruction radius, r_d varies with core luminosity. As a first approximation, the dust destruction radius will vary as

$$L = Ar_d^2 \quad (\text{A3})$$

for some constant A . Table 3 of Wolfire & Cassinelli (1987) suggests that $A \approx 3 \times 10^8 \text{ erg s}^{-1} \text{ cm}^{-2}$. If it is assumed that equation A3 is an expression of the Stefan–Boltzmann Law, then the implied temperature is less than 1000 K - far below the nominal dust melting temperature, and another example of the importance of the wavelength dependence of the dust opacity. However, with this dependence folded into A , equation A3 may be safely used to estimate the value of r_d .

Putting this together with the free fall assumption yields

$$\dot{M}\sqrt{2GM_*} > \frac{L^{\frac{5}{4}}}{c^{\frac{3}{4}}A}$$

or

$$4\dot{M}^4G^2M_*^2 > \frac{L^5}{Ac^4} \quad (\text{A4})$$

Substituting an accretion luminosity then yields

$$\dot{M} < 4G^{-3}M_*^{-3}R_*^5Ac^4$$

Finally, putting in the mass-radius relation gives

$$\dot{M} < \frac{4AR_\odot^5c^4}{G^3M_\odot^3} \sim 6 M_\odot \text{ yr}^{-1} \quad (\text{A5})$$

as the condition for accretion. Rather surprisingly, this is independent of the stellar mass. However, no star of reasonable mass could accrete at this rate and remain on the main sequence. We therefore conclude that accretion luminosity on its own is unlikely to shut down an accretion flow.

A2 Luminosity Dominated by Nuclear Burning

If the luminosity is dominated by nuclear reactions in the core, a different relation between L and M is obtained. For main sequence stars, $L \sim M^\psi$, where ψ is in the range of two to three for most stars (although the most massive stars have $\psi \sim 1$). Substituting the power law relation into equation A4 suggests that the condition on the accretion rate will become

$$\dot{M}^4 > \frac{L_\odot^5}{4G^2Ac^4M_\odot^{5\psi}}M_*^{5\psi-2} \quad (\text{A6})$$

Within the likely range of values for ψ , this *minimum* accretion rate is a rather rapidly increasing function of M_* .

Hence, accretion is becoming harder, and is likely to shut down.

ACKNOWLEDGMENTS

The authors would like to thank Jim Pringle and Ian Bonnell for several useful discussions. RGE is also particularly grateful to Matthew Bate, for his aid with ZEUS. Chris Tout kindly supplied his ZAMS formulae and information on possible accretion rates.

REFERENCES

- Bell K. R., Cassen P. M., Klahr H. H., Henning T., 1997, *ApJ*, 486, 372
- Bodenheimer P., Yorke H. W., Rozyczka M., Tohline J. E., 1990, *ApJ*, 355, 651
- Bonnell I. A., Bate M. R., Zinnecker H., 1998, *MNRAS*, 298, 93
- Braun J. M., Bomans D. J., Will J., de Boer K. S., 1997, *A&A*, 328, 167
- Draine B. T., Lee H. M., 1984, *ApJ*, 285, 89
- Draine B. T., Malhotra S., 1993, *ApJ*, 414, 632
- Duschl W. J., Gail H.-P., Tscharnuter W. M., 1996, *A&A*, 312, 624
- Gail H.-P., Sedlmayr E., 1999, *A&A*, 347, 594
- Garay G., Lizano S., 1999, *PASP*, 111, 1049
- Krueger D., Gauger A., Sedlmayr E., 1994, *A&A*, 290, 573
- Laor A., Draine B. T., 1993, *ApJ*, 402, 441
- Larson R. B., 1969, *MNRAS*, 145, 271
- Larson R. B., Starrfield S., 1971, *A&A*, 13, 190
- Lenzuni P., Gail H., Henning T., 1995, *ApJ*, 447, 848
- Mathis J. S., Rimpl W., Nordsieck K. H., 1977, *ApJ*, 217, 425
- Mendoza E. E., 1968, *ApJ*, 151, 977
- Nakano T., 1979, *PASJ*, 31, 697
- Olsen K. A. G., Kim S., Buss J. F., 2001, *AJ*, 121, 3075
- Penston M. V., 1969, *MNRAS*, 144, 425
- Preibisch T., Ossenkopf V., Yorke H. W., Henning T., 1993, *A&A*, 279, 577
- Preibisch T., Sonnhalter C., Yorke H. W., 1995, *A&A*, 299, 144
- Pringle J. E., 1981, *ARA&A*, 19, 137
- Safier P. N., McKee C. F., Stahler S. W., 1997, *ApJ*, 485, 660
- Shu F. H., Adams F. C., Lizano S., 1987, *ARA&A*, 25, 23
- Stahler S. W., Palla F., Ho P. T. P., 2000, *Protostars and Planets IV*, p. 327
- Stone J. M., Norman M. L., 1992, *ApJS*, 80, 753
- Tenorio-Tagle G., Bodenheimer P., Lin D. N. C., Noriega-Crespo A., 1986, *MNRAS*, 221, 635
- Tout C. A., Livio M., Bonnell I. A., 1999, *MNRAS*, 310, 360
- Tout C. A., Pols O. R., Eggleton P. P., Han Z., 1996, *MNRAS*, 281, 257
- Wolfire M. G., Cassinelli J. P., 1986, *ApJ*, 310, 207
- Wolfire M. G., Cassinelli J. P., 1987, *ApJ*, 319, 850
- Yorke H. W., 1979, *A&A*, 80, 308
- Yorke H. W., 1980, *A&A*, 85, 215
- Yorke H. W., Bodenheimer P., 1999, *ApJ*, 525, 330
- Yorke H. W., Bodenheimer P., Laughlin G., 1993, *ApJ*, 411, 274
- Yorke H. W., Bodenheimer P., Laughlin G., 1995, *ApJ*, 443, 199
- Yorke H. W., Sonnhalter C., 2002, *ApJ*, 569, 846

This paper has been typeset from a $\text{\TeX}/\text{\LaTeX}$ file prepared by the author.